

# Electrically-controlled two-dimensional gratings based on layers undulations in cholesteric liquid crystals

Bohdan Senyuk<sup>1,\*</sup>, Ivan Smalyukh<sup>2</sup>, Oleg Lavrentovich<sup>1,2,#</sup>

<sup>1</sup>Chemical Physics Interdisciplinary Program and <sup>2</sup>Liquid Crystal Institute,  
Kent State University, Kent, OH, USA 44242-0001

## ABSTRACT

We developed electrically-switchable two-dimensional diffractive gratings with periodic refractive index modulation arising from layers undulations in cholesteric liquid crystal. Two-dimensional layer undulations occur above the threshold voltage when a planar cholesteric cell of thickness much larger than the cholesteric pitch is subjected to an electric field. The periodic structure of the layers undulations and corresponding spatial modulation of an average refractive index in the plane of a cell allows us to produce diffraction patterns with a square-type arrangement of diffraction maxima. The cholesteric cell can be switched by pulses of ac voltage between two states: one with flat layers of a planar cholesteric texture and another with square lattice of periodic director modulation associated with layer undulations that produces two-dimensional diffraction patterns. The periodicity of the developed two-dimensional phase gratings and intensities of the diffraction maxima can be tuned by changing the applied field magnitude. The diffractive properties of gratings are practically independent of the polarization state of the incident beam and can be optimized for different wavelengths by appropriately choosing the cholesteric pitch, cell thickness, and surface treatment. The potential applications include beam steering devices, optical waveguides, devices for splitting monochromatic beams and beam multiplexing.

**Keywords:** liquid crystals, cholesterics, phase gratings

## 1. INTRODUCTION

Electrically-controlled phase gratings are widely used in optics for beam steering, optical waveguides, and splitting monochromatic beams. They have also become very popular for local beam multiplexing for optical multi-beam devices. Splitting the beam into a given number of beams by using of a two-dimensional (2D) grating is an efficient way to distribute the local source power to an array of receivers. Liquid crystal (LC) devices have a great potential as electrically switchable 2D diffraction gratings. The simplest 2D grating can be produced by orthogonally overlaying two one-dimensional (1D) structures<sup>1</sup>. This results in a rectangular diffraction pattern and the grating efficiency is then a product of the efficiencies of two 1D gratings.<sup>1</sup> Another approach employs ordered LC droplet structures<sup>2,3</sup> in which the diffraction pattern is switched by changing the director field in the droplets. 2D diffraction can be also produced using a spatial light modulator<sup>4</sup>. However, all of these approaches are either technologically challenging or produce comparably small diffraction efficiency. On the other hand, 1D electrically-controlled gratings based on periodically-modulated textures in thin cholesteric cells<sup>5-9</sup> as well as polymer-stabilized,<sup>10</sup> polymer dispersed,<sup>11</sup> and photocurable<sup>12</sup> LC gratings offer technological simplicity and good diffraction quality. In this paper we propose electrically-controlled 2D gratings<sup>13</sup> that employ the layers undulations in cholesteric LCs which can work in both Raman-Nath and Bragg regimes. We demonstrate that the spatial periodicity of the diffraction pattern can be changed and adjusted for different wavelengths by using cholesterics of different pitch and by confining them into cells of different thickness. Also, the undulation periodicity can be continuously tuned by the applied voltage and the grating can be switched between the diffraction and no-diffraction states using pulses of ac voltage. The present 2D cholesteric grating can be controlled by low voltages; this assures low power consumption of the device.

---

\* Email bohdan@lci.kent.edu; Phone 1-330-672-1518

# Email odl@lci.kent.edu; Phone 1-330-672-4844

## 2. EXPERIMENTAL

### 2.1. Cell preparation and materials

The LC cells for 2D cholesteric gratings (Fig. 1) were constructed from glass substrates coated with transparent indiumtin-oxide (ITO) patterned electrodes. The unidirectionally buffed thin layers of polyimide PI2555 (HD MicroSystem) were used to set the easy axis for LC molecules at the confining glass plates; we used different rubbing strength (between 7÷15 rubbings with pressure  $\approx 827.37 \text{ Pa}$ ) in order to get different surface anchoring strength. Also, the orientation of the rubbing directions on the opposite substrates was anti-parallel and orthogonal. The cell thicknesses varied in the range  $d = 10 - 60 \mu\text{m}$  and was set using the glass spacers uniformly mixed with UV-light sensitive glue placed at the cell edges. The actual thickness  $d$  after the cell assembly was measured using the interference method and spectrophotometer Lambda18 (Perkin Elmer). In the LC mixtures (Table 1) the cholesteric pitch  $p$  was varied from values much larger than wavelength of the incident laser beam ( $p \gg \lambda$ ) to much smaller values ( $p < \lambda$ ). The nematic hosts E7, 5CB, ZLI-3412 were doped with a chiral agent CB15 and the nematic host BL015 was doped with a chiral dopant ZLI-811 (all from EM Industries). The cholesteric mixtures were additionally doped with  $\sim 0.01\%$  of fluorescent dye N,N'-Bis(2,5-di-tert-butylphenyl)-3,4,9,10-perylenedicarboximide (BTBP) for the Fluorescence Confocal Polarizing Microscopy (FCPM) observations.<sup>14</sup> To minimize spherical aberrations in the FCPM<sup>14</sup> observations with the immersion oil objectives, we used glass plates of thickness  $0.15 \text{ mm}$  with refractive index 1.52.

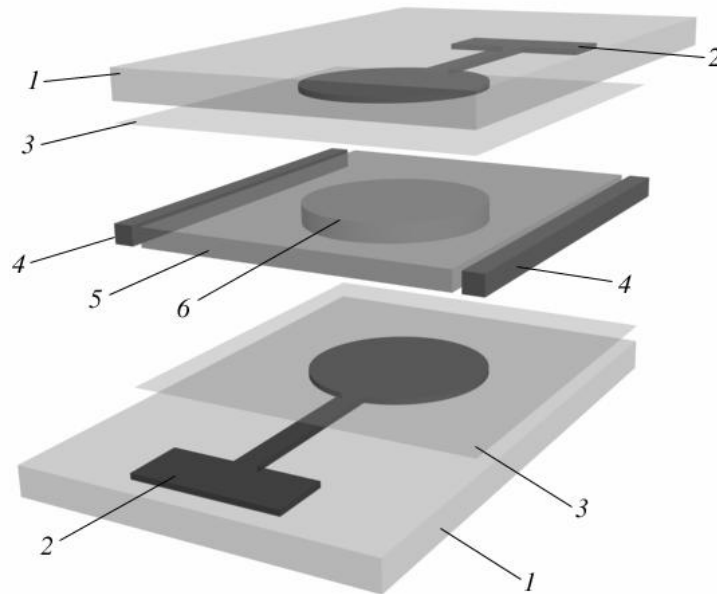


Fig. 1. Design of cholesteric liquid crystal grating: 1 – glass substrates; 2 – transparent patterned electrodes; 3 – alignment film; 4 – spacers; 5 – cholesteric liquid crystal; 6 – working area with layers undulations.

Table 1. Liquid crystal materials and their electro-optic characteristics.

Nematic host	Optical anisotropy of nematic host, $\Delta n$	Dielectric anisotropy of nematic host, $\Delta \epsilon$	Chiral dopant, % by weight	Pitch, $\mu\text{m}$
E7	0.224	13.8	CB15, $\sim 2.7\%$	5.0
5CB	0.211	11.5	CB15, $\sim 2.8\%$	5.0
ZLI-3412	0.078	3.4	CB15, $\sim 3.2\%$	5.0
BL015	0.28	16	ZLI-811, $\sim 30\%$	0.31

The LC cells (Fig. 1) were filled with cholesteric mixtures (Table 1) in the isotropic state and then slowly ( $0.5 \text{ degree/min}$ ) cooled down. After the system relaxed the cells with uniform planar cholesteric structure free of defects were obtained (Fig. 1). An ac voltage ( $1 \text{ kHz}$ ) was applied using the generator DS345 (Stanford Research Systems) and the wideband amplifier 7602 (Krohn-Hite).

Experimental polarizing microscopy (PM) observations were performed using the Nikon Eclipse E600 POL microscope. The PM textures were acquired using the Hitachi HV-C20 CCD camera. The studies of director field of the layered structure were performed using the modified BX-50 Olympus microscope in the FCPM<sup>14</sup> mode. The Ar laser ( $\lambda = 488 \text{ nm}$ ) was used for excitation of the BTBP and the fluorescent light was detected in the spectral range  $510 - 550 \text{ nm}$ .

## 2.2. Layers undulations in cholesteric liquid crystals

When strongly twisted ( $d/p \gg 1$ ), cholesterics can be described as lamellar phases<sup>15-17</sup> with thickness of the layer set by cholesteric pitch and equal  $p/2$ . Similarly to other lamellar media (smectics,<sup>18</sup> block copolymers,<sup>19</sup> and others), the layers undulations can be produced by various external factors: mechanical dilatation,<sup>18</sup> changing temperature, magnetic<sup>20,21</sup> or electric fields.<sup>22,23</sup> When no field is applied, the helical axis is perpendicular to bounding plates and the average refractive index is uniform in the plane of a cell. In the applied electric field, the LC molecules and, respectively, cholesteric layers tend to reorient along the field. When the voltage reaches some critical value, the layers undulations occur<sup>22,23</sup> (Fig. 2) as a compromise between the dielectric and surface energies. In the studied cells with  $d/p > 2.5$ , the 2D patterns of undulations appear at the threshold voltage  $U_u = 3 - 15 \text{ V}$ . The two mutually orthogonal wave vectors of the patterns are at  $45^\circ$  to the rubbing directions in the cells with substrates rubbed in perpendicular fashion. In the cells with anti-parallel rubbing, one of the wave vectors is parallel to the rubbing and another is perpendicular to it. The difference between the spatial periods of undulations in two orthogonal directions is less than 1% (Fig. 2). The amplitude of undulations  $u_0$  scales as  $(E^2/E_c^2 - 1)^{1/2}$ , where  $E$ ,  $E_c$  are applied electric field and critical electric field, respectively.<sup>24</sup> The period of the square lattice  $L_u$  can be varied in the submicron-micron range (Fig. 2) by adjusting  $d$ ,  $p$ , and surface treatment (different types of the alignment layer, different rubbing strength).<sup>13</sup> The patterns of undulations (Fig. 2) correspond to 2D spatial modulation of director, phase retardation, and the effective refractive index. Fig. 2 shows the uniform PM textures of undulations in the cholesteric LC cell with different ratio  $d/p$ .

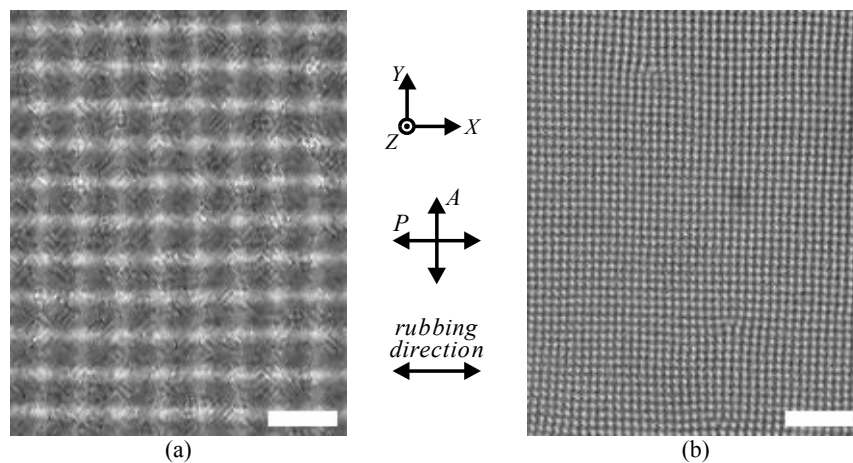


Fig. 2. Polarizing-microscopy textures of the 2D undulations in cholesteric cells under applied ac voltage  $U$  ( $1 \text{ kHz}$ ): (a) 5CB+CB15,  $p = 5 \mu\text{m}$ ,  $d/p \approx 2.5$ ,  $U = 3.6 \text{ V}$ ; (b) BL015 + ZLI-811,  $p = 0.31 \mu\text{m}$ ,  $d/p \approx 40$ ,  $U = 14 \text{ V}$ . Scale bar is  $20 \mu\text{m}$ .

## 2.3. Oily streaks and patterned electrodes

In the development of the phase gratings based on the undulations, there was a problem that before the 2D layers undulations develop one often observes defects called oily streaks.<sup>25</sup> The appearance of this type of defects is a nucleation process<sup>25</sup> and, usually the irregularities of the orientation at the edges of the cell are the nuclei for appearance

of oily streaks (Fig. 3). In order to prevent nucleation at the cell edges, the transparent electrodes were patterned (Fig. 1) with the working area being  $25 \text{ mm}^2$ . This allows us to avoid the oily streaks by eliminating the nucleation sites such as surface irregularities, mechanical impurities, and strong layers distortions at the cell edges. The obtained 2D undulations were stable in time without being spoiled by the oily streaks.

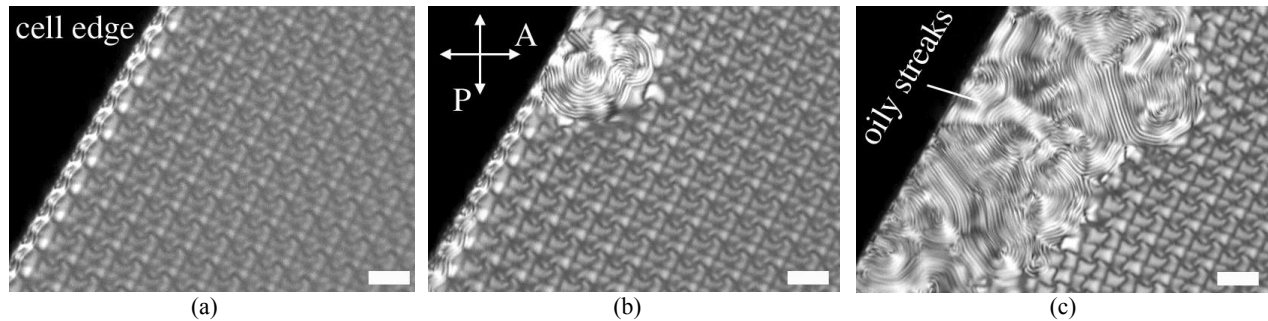


Fig. 3. Nucleation of oily streaks at the liquid crystal cell edge caused by orientation irregularities near the sealing wall: (a) undulation pattern at the onset of undulations; (b) nucleation of oily streaks; (c) expansion of oily streaks through the cholesteric cell. The scale bar is  $20 \mu\text{m}$ .

### 3. EXPERIMENTAL RESULTS AND DISCUSSION

#### 3.1. Diffraction patterns

We studied the diffraction parameters using a setup consisting of an Ar laser ( $\lambda = 488 \text{ nm}$ ), a polarizer, a quarter-wave plate, the cholesteric cell, and a screen. A photodetector was used to measure the intensity for each maximum of the diffraction pattern (Fig. 4). The combination of a polarizer and a quarter-wave plate allowed us to tune the polarization

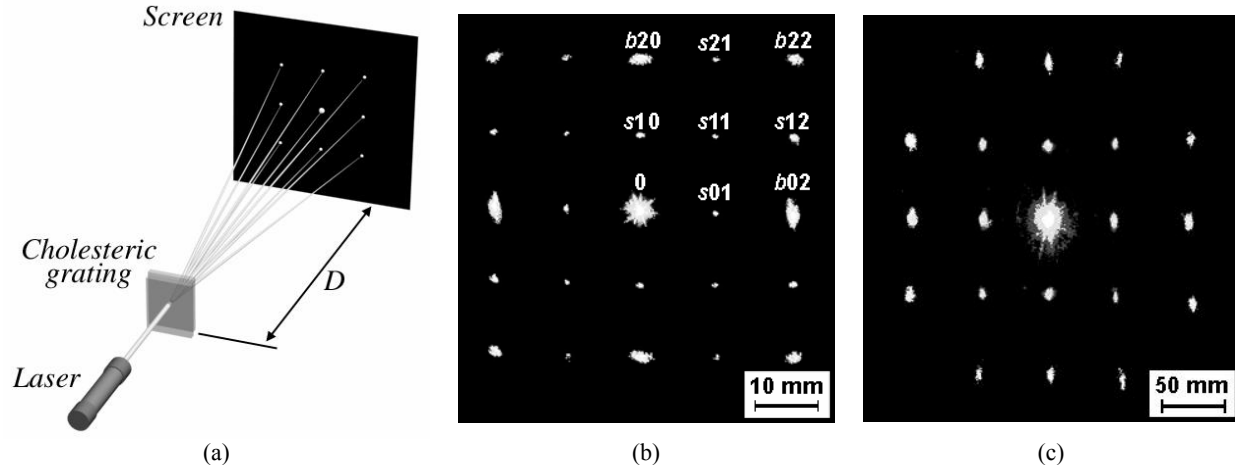


Fig. 4. (a) Setup for the experimental study of cholesteric gratings and diffraction patterns obtained for cholesteric cells with: (b) mixture of 5CB+CB15,  $p = 5 \mu\text{m}$ ,  $d/p \approx 2.5$ ,  $U = 3.6 \text{ V}$  and (c) mixture of BL015 + ZLI-811,  $p = 0.31 \mu\text{m}$ ,  $d/p \approx 40$ ,  $U = 14 \text{ V}$ . Distance from the cholesteric grating to the screen is  $D = 0.25 \text{ m}$ .

state of the incident light from linear to circular and thus to study the dependence of the diffraction patterns on the light polarization. The diffraction angle  $\theta$  for the first diffraction maximum was in the range  $\theta = 1 - 15^\circ$  for the Ar-laser beam and up to  $42^\circ$  for an infrared beam at  $\lambda \approx 3 \mu\text{m}$  (tunable diode laser, Laser Components Instrument Group), depending on  $d$  and  $p$ . The observed diffraction pattern is well described by the diffraction condition for maximum intensity:

$$m\lambda = L_g \sin \theta \quad (1)$$

where  $m$  is the diffraction order, and  $L_g$  is the grating periodicity. The positions of the intensity maxima satisfy the equations

$$r = \lambda D(m_x^2 + m_y^2)^{1/2}/L_g, \quad \tan \varphi = m_y/m_x \quad (2)$$

where  $r$  is the distance from the center to the intensity maximum,  $m_x$  and  $m_y$  are the diffraction orders in the  $X$  and  $Y$  directions,  $\varphi$  is the angle between the  $X$ -axis and the vector connecting the 0-th and  $m$ -th diffraction maxima, and  $D$  is the distance to the screen.

The diffraction pattern strongly depends on the ratio  $d/p$ . For cells with  $2.5 < d/p < 10$ , the intensities of the odd and even diffraction maxima are non-monotonic functions of  $m_x$ ,  $m_y$  (Fig. 4(b)) similarly to the case of 1D cholesteric gratings.<sup>6</sup> The cells with  $d/p > 10$  produce diffraction patterns in which the intensities of maxima monotonically decrease with the increase of the diffraction order (Fig. 4(c)). Clearly, the “odd-even” effect is a feature of the 2D gratings with comparably small number of layers,  $d/p < 10$ , and is not present for relatively thick samples of  $d/p > 10$ .

### 3.2. FCPM observations and spatial distribution of refractive index in gratings

In order to get an insight into the “odd-even” effect we use the FCPM<sup>14</sup> for imaging of the director in the vertical cross-sections of cells (Fig. 5). The cholesteric layer that is adjacent to the substrate is not flat indicating that cholesteric anchoring is finite.<sup>21,24</sup> One can distinguish two different types of spatial distortions of the LC director and the average

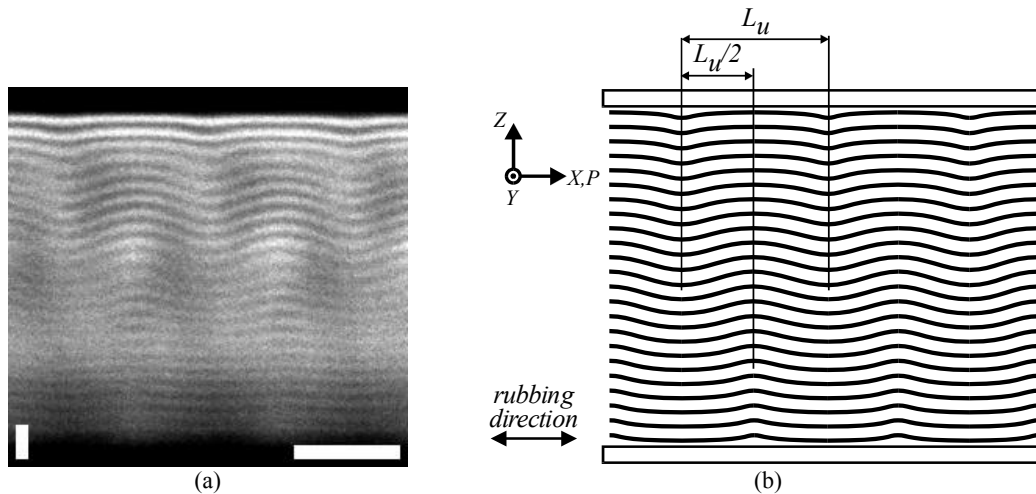


Fig. 5. FCPM cross-section of 2D undulations in the cholesteric cell with a mixture of ZLI-3412+CB15 ( $p = 5 \mu\text{m}$ ,  $d/p \approx 11$ ,  $U = 12 \text{ V}$ ) (a) and the reconstructed layers pattern (b). “ $P$ ” marks the polarization direction of probing light in FCPM. Horizontal scale bar is  $20 \mu\text{m}$ ; vertical scale bar is  $5 \mu\text{m}$ .

refractive index: one in the bulk region and another at the two surface regions. The modulation of the refractive index scales as  $(\partial u/\partial x)^2$ , where  $u$  is the displacement of layers from their unperturbed flat positions and  $\partial u/\partial x$  is the layers tilt with respect to the substrate. Therefore, the grating in (Fig. 5(a)) can be qualitatively considered as comprised of three adjacent parts: two gratings created by the close-to-surface layers at the confining substrates with the period of the refractive index  $L_g = L_u$ , and the LC bulk grating with the period of the refractive index  $L_g = L_u/2$ . The two surface gratings are shifted by  $L_u/2$  with respect to each other and separated by the distance  $\sim d$  along the  $Z$ -axis. The resulting diffraction pattern is a superposition of diffraction effects due to the three stacked gratings and can be described using equations (1) and (2). The diffracted beams “ $b$ ” (Fig. 4(b)) are caused by modulation of refraction index in the bulk with

period  $L_u/2$  and the beams “s” (Fig. 4(b)) are caused by modulation of refractive index close to surfaces with period  $L_u$ . When  $d/p$  is large, the contribution from the regions close to the surfaces is negligible as compared to the modulation of the refractive index in the bulk of the cell and the diffraction maxima caused by the near-to-surface layers are not observed (Fig. 4(c)). Thus, the alternation of strong- and weak-intensity maxima in the diffraction pattern is caused by the surface confinement, similarly to the case of 1D cholesteric gratings.<sup>6</sup>

### 3.3. Characterization of diffraction patterns

Changing the applied voltage leads to changing of the layers displacement  $u_0$ ; the layers undulations become more or less pronounced and, as a consequence, the depth of the modulation of the effective refractive index changes too. Therefore, the intensities of the high-order maxima can be controlled with the voltage (Fig. 6). Importantly, the performance of the gratings was found to be practically polarization-independent and the relative intensities of the diffraction maxima did not change much after switching the linear polarization state between the two orthogonal directions (up to 5 %) or changing polarization from linear to circular (up to 10 %). The diffraction pattern is stable in the wide voltage range. For example, 55  $\mu\text{m}$  thick cells with E7+CB15 mixture of pitch  $p = 5 \mu\text{m}$  produce the diffraction pattern within the voltage range  $U = 12 - 25 \text{ V}$  in which one can control the intensities of the high order maxima (Fig. 7).

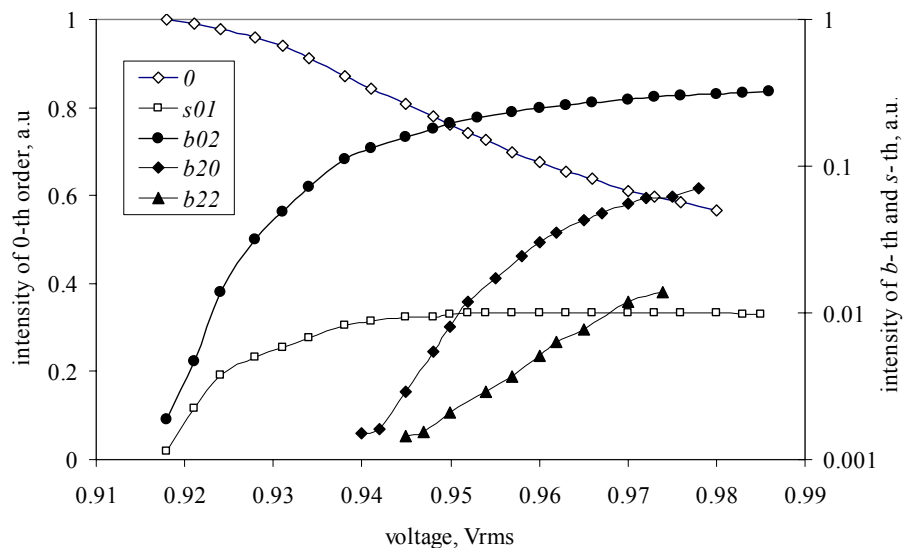


Fig. 6. Intensities for different order diffraction maxima vs. voltage for the cholesteric cell with cell thickness  $d = 12.5 \mu\text{m}$  and pitch  $p = 5 \mu\text{m}$ .

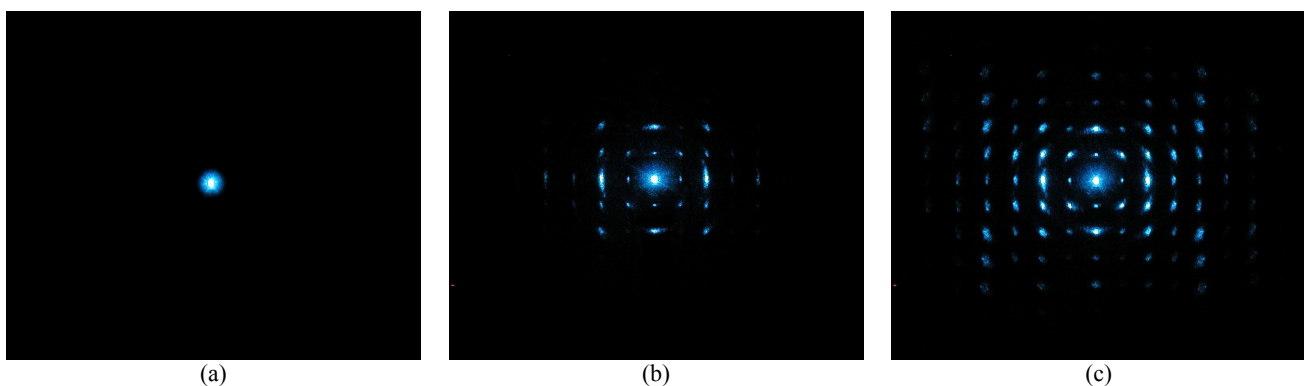


Fig. 7. Control of the diffracted beams pattern with applied voltage (5CB+CB15, pitch  $p = 5 \mu\text{m}$ ,  $d/p \approx 2.5$ ): (a)  $U = 0 \text{ V}$ ; (b)  $U = 3.6 \text{ V}$ ; (c)  $U = 6 \text{ V}$ .

We observed and characterized the dependence of the spatial periods  $L_u$  of the 2D layers undulations lattice on the applied field (Fig. 8). When the applied voltage was increased the undulations period increased equally in both directions. Increasing of the undulation periods  $L_u$  is implemented via appearance and movement of dislocations in the square lattice of undulations which does not affect much diffraction patterns and diffraction efficiency. This study shows the possibility to design 2D gratings with voltage tunable spatial periodicity.

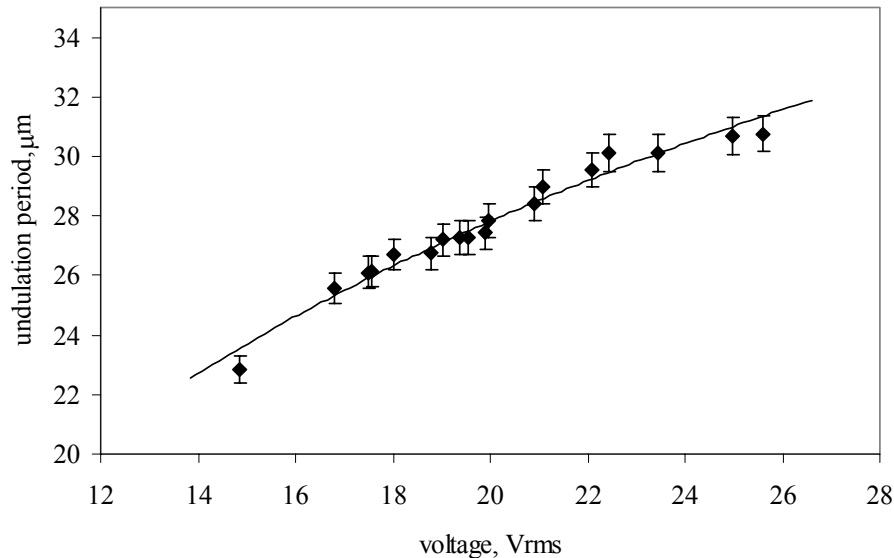


Fig. 8. Dependence of the undulation period on applied voltage for the cholesteric cell with  $d = 50 \mu\text{m}$  and  $p = 5 \mu\text{m}$ .

Depending on the parameter  $\kappa = \lambda d/L_g^2$ , one can distinguish the Raman-Nath ( $\kappa \ll 1$ ) and Bragg ( $\kappa > 1$ ) types of diffraction.<sup>26</sup> The layers undulations in cholesteric cell can be used as gratings of both types. The conditions for the Bragg diffraction are achievable, especially with small  $p$  and  $\lambda$  in the infrared region. For example, for  $p = 0.31 \mu\text{m}$  and  $\lambda = 3 \mu\text{m}$  one obtains  $\kappa$  which corresponds to the Bragg diffraction regime. In the opposite limit, a thin grating with  $d = 12.5 \mu\text{m}$  and  $p = 5 \mu\text{m}$  produces diffraction in the Raman-Nath regime at  $\lambda = 0.488 \mu\text{m}$ . We refer the reader to Ref.[13] for more detailed discussion of this subject.

The switching between the 1D and 2D diffraction grating can be achieved in the cholesteric cells with  $2 < d/p < 2.5$  (Fig. 9). First, at some threshold voltage there is the 1D layers undulations (Fig. 9(a)) that produce the 1D diffraction pattern (Fig. 9(c)), and, when the voltage achieves some second threshold value, the 1D layers instability transforms into 2D layers undulations (Fig. 9(b)) that produce the diffraction pattern with square-type arrangement of diffracted beams (Fig. 9(d)).

#### 4. CONCLUSIONS

To summarize, we demonstrated that the layers undulations in the cholesteric cells can be used as switchable weakly polarization dependent 2D diffraction gratings of both Raman-Nath and Bragg types. The periodic structure of the layers undulations and corresponding spatial modulation of an average refractive index in the plane of a cell allows us to produce diffraction patterns with a square-type arrangement of diffraction maxima. The spatial periodicity of the diffraction pattern can be changed and adjusted for different wavelengths by using cholesterics of different pitch and by confining them into cells of different thickness. The intensities of diffraction maxima can be continuously tuned by the applied voltage; the grating can be switched between the diffraction and no-diffraction states using pulses of ac voltage. The value of the surface anchoring influences the critical field needed for layers undulations appearance. We also demonstrated that the voltage tunable 2D diffraction gratings of variable spatial periodicity can be designed employing

the effect of layers undulations in cholesteric LCs. The switching between the 1D and 2D diffraction gratings is possible within some range of parameters of the cholesteric LC cell.

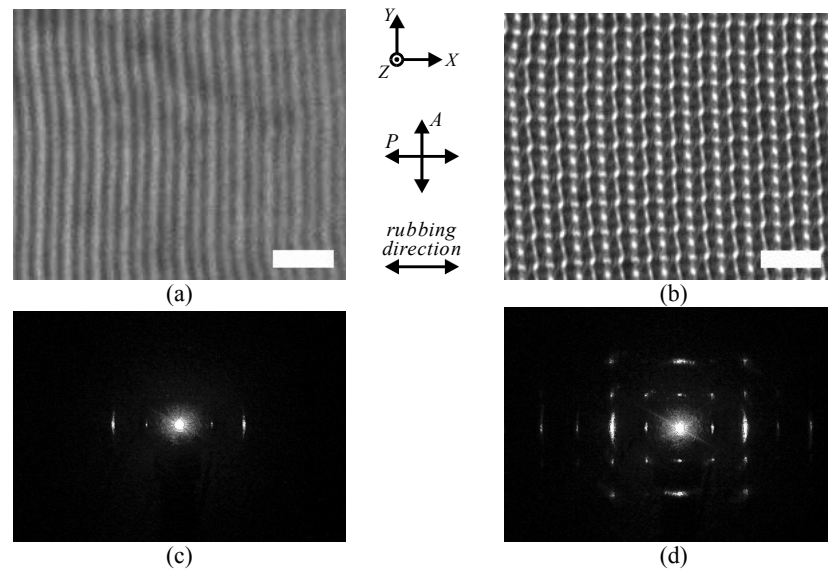


Fig. 9. Switching between the 1D and 2D diffraction gratings (E7+CB15,  $p = 5 \mu\text{m}$ ,  $d/p \approx 2.3$ ): (a) 1D layers undulations texture ( $U = 4.3 \text{ V}$ ); (b) 2D layers undulations texture ( $U = 4.45 \text{ V}$ ); (c) 1D diffraction pattern; (d) 2D diffraction pattern. Scale bar is  $20 \mu\text{m}$ .

## ACKNOWLEDGMENTS

Work was partially supported by the National Science Foundation, Grant DMR-0315523. Authors thank A. Glushchenko, M. Kleman, L. Longa, Yu. Nastyshyn, V. Nazarenko, and V. Pergamenschik for fruitful discussions. B.I.S. acknowledges the 2004 SPIE Educational Award.

## REFERENCES

1. P. F. McManamon, T. A. Dorschner, D. L. Corkum, L. J. Friedman, D. S. Hobbs, M. Holz, S. Liberman, H. Q. Nguyen, D. P. Resler, R. C. Sharp, E. A. Watson, "Optical phased array technology," *Proceedings of the IEEE*, **84**(2), 268-298, 1996.
2. A. Fernandez-Nieves, D. R. Link, D. Rudhardt, D. A. Weitz, "Electro-optics of bipolar nematic liquid crystal droplets," *Phys. Rev. Lett.* **92**, 105503/1-4, 2004.
3. D. Rudhardt, A. Fernandez-Nieves, D.R. Link, and D.A. Weitz, "Phase switching of ordered arrays of liquid crystal emulsions," *Appl. Phys. Lett.* **82**(16), 2610-2612, 2003.
4. E. Schulze and Wolf von Reden, "Diffractive liquid crystal spatial light modulators with optically integrated fine-pitch phase gratings," in *Liquid Crystal Materials, Devices, and Displays*, R. Shashidhar, U. Efron, eds., *Proc. SPIE* **2408**, 113-120, 1995.
5. D. Subacius, P. J. Bos and O. D. Lavrentovich, "Switchable diffractive cholesteric gratings," *Appl. Phys. Lett.* **71**(10), 1350-1352, 1997.
6. S. V. Shiyankovskii, D. Subacius, D. Voloschenko, P. J. Bos, O. D. Lavrentovich, "Cholesteric diffraction devices with a field-controlled grating vector," in *Liquid Crystals II*, I.-C. Khoo, ed., *Proc. SPIE* **3475**, 56-64, 1998.
7. O. D. Lavrentovich, S. V. Shiyankovskii, and D. Voloschenko, "Fast beam steering cholesteric diffractive devices," in *Optical Scanning: Design and Application*, L. Beiser, Stephen F. Sagan, G. F. Marshall, eds., *Proc. SPIE* **3787**, 149-155, 1999.
8. O. D. Lavrentovich, D. Subacius, "Diffraction grating with electrically controlled periodicity," U.S. Patent 6188462 B1, 2001.
9. D. Subacius, S. V. Shiyankovskii, Ph. Bos and O. D. Lavrentovich, "Cholesteric gratings with field-controlled period," *Appl. Phys. Lett.* **71**(23), 3323-3325, 1997.
10. S. W. Kang, S. Sprunt, and L. C. Chien, "Structure and morphology of polymer-stabilized cholesteric diffraction gratings," *Appl. Phys. Lett.* **76**(24), 3516-3518, 2000.
11. Andy Y.-G. Fuh, M.-S. Tsai, L.-J. Huang and T.-C. Liu, "Optically switchable gratings based on polymer-dispersed liquid crystal films doped with a guest-host dye," *Appl. Phys. Lett.* **74**(18), 2572-2574, 1999.



12. Anup K. Ghosh, Yoichi Takanishi, Ken Ishikawa, and Hideo Takezoe, Youshiyuki Ono, Joji Kawamura, "Electrically controllable polarization-dependent phase grating from photocurable liquid crystals," *J. Appl. Phys.* **95**(9), 5241-5243, 2004.
13. B. I. Senyuk, I. I. Smalyukh, O. D. Lavrentovich, "Switchable two-dimensional gratings based on field-induced layer undulations in cholesteric liquid crystals," *Opt. Lett.* **30**(4), 349-351, 2005.
14. I. I. Smalyukh, S. V. Shiyankovskii, and O. D. Lavrentovich, "Three-dimensional imaging of orientational order by fluorescence confocal polarizing microscopy," *Chem. Phys. Lett.* **336**, 88-96, 2001.
15. T. S. Lubensky, "Hydrodynamics in cholesteric liquid crystals," *Phys. Rev. A* **6**, 452-470, 1972.
16. P.G. de Gennes and J. Prost, *Physics of Liquid Crystals*, 2nd ed., Clarendon Press, Oxford, 1992.
17. M. Kleman, O. D. Lavrentovich, *Soft Matter: An Introduction*, p.450, Springer, New-York, 2003.
18. N. A. Clark, R. B. Meyer, "Strain-induced instability of monodomain smectic A and cholesteric liquid crystals," *Appl. Phys. Lett.* **22**(10), 493-494, 1973.
19. Z.-G. Wang, "Response and instabilities of the lamellar phase of diblock copolymers under uniaxial stress," *J. Chem. Phys.* **100**(3), 2298-2309, 1994.
20. J. P. Hurault, "Static distortions of a cholesteric planar structure induced by magnetic or ac electric fields," *J. Chem. Phys.* **59**(4), 2068-2075, 1973.
21. T. Ishikawa, O. D. Lavrentovich, "Undulations in a confined lamellar system with surface anchoring," *Phys. Rev. E* **63**, 030501(R)/1-3, 2001.
22. W. Helfrich, "Deformation of cholesteric liquid crystals with low threshold voltage," *Appl. Phys. Lett.* **17**(12), 531-532, 1970.
23. W. Helfrich, "Electrohydrodynamic and dielectric instabilities of cholesteric liquid crystals," *J. Chem. Phys.* **55**(2), 839-842, 1971.
24. B. I. Senyuk, I. I. Smalyukh, O. D. Lavrentovich, *in preparation*.
25. O. D. Lavrentovich, D.-K. Yang, "Cholesteric cellular patterns with electric-field-controlled line tension," *Phys. Rev. E* **57**(6), R6269-R6272, 1998.
26. R.W. Boyd, *Nonlinear Optics*, p.318, Academic, San Diego, 1992.